Monografías Matemáticas *García de Galdeano* **41**, 117–130 (2018)

The regular polygon problem of $(N+1)$ bodies: the past, the present and the future

Tilemachos J. Kalvouridis

Abstract. We deal with the dynamics of a small body, either natural or artificial, acted upon by the gravitational forces of a coplanar system of N big bodies, the $\nu = N - 1$ of which have equal masses m and are located at the vertices of a regular ν-gon, while the Nth body with a different mass m_0 is located at the center of mass of the system. Our aim is to present an overview of the main results obtained so far from the study of the original configuration and of various versions of the dynamical system, together with a brief reference to our recent work and to our projects in progress.

Keywords: Regular polygon problem of $(N + 1)$ bodies.

§1. Introduction

The Newtonian general N-body problem has historically served as a source of inspiration and creation of new problems of Celestial Mechanics but it still remains unsolved in the sense that we are not able to find closed mathematical solutions of it. However serious efforts are done on the direction of studying simpler models of more than two bodies even since the era of Lagrange and Euler and find particular solutions. The famous restricted three-body problem is one of them. A relatively new model is the regular polygon problem of $(N + 1)$ bodies [31, 16], etc. It deals with the dynamics of a small body moving in the force field created by N big bodies the $\nu = N - 1$ of which with equal masses are located at the vertices of a regular ν-gon, while the Nth body with a different mass is located at the center of mass of the system. The geometric formation of the big bodies is based on a model proposed in 1865 by Maxwell in order to explain the rings of Saturn. Ever since, many papers concerning the above problem, appeared in the international bibliography [18, 19, 21, 7, 8, 9, 5, 15, 6, 29, 23], etc. Here we note that in the past, this configuration was used as a cosmological model, as a mechanism to describe the concentration of interplanetary matter in the neighborhood of planetary systems and of the creation of proto-nebulae, as well as a simplified model to describe co- orbital or quasi co-orbital systems of astronomical objects (asteroids, moons, or natural satellites) orbiting at almost the same, distance from their primary. Finally, it was proposed to simulate the rings observed around the giant planets of our solar system. The configuration we are dealing with is a central one, meaning that the resultant force acting on each body of the system is always directed to a fixed center. A particular class of solutions is the homographic ones where the configuration remains always similar to itself and a sub-class consists of the relative equilibria. These solutions were investigated among others by [30, 33],

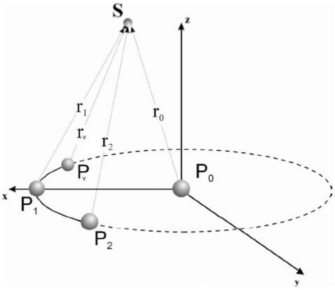

(a)

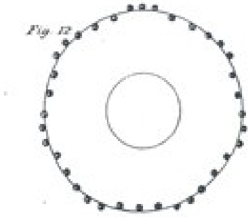

(b)

Figure 1: (a) The configuration of the classical regular polygon problem of $(N + 1)$ bodies, (b) Maxwell's sketch of his proposed model (1857).

etc., while Arribas et al. [3, 4] studied some cases with quasi-homogeneous potentials. The next two paragraphs refer to the original gravitational problem and the various versions of it respectively, while in the last paragraph we present some recent results and we expose some new ideas for further improvement and generalization of the initial model, on which we are already working on.

§2. Dynamics of a small body in a regular polygon configuration of N bodies and some results obtained so far from the study of the classical gravitational case

The original gravitational version is characterized with two parameters; the number of the peripheral bodies $\nu = N - 1$ and the mass parameter $\beta = m_0/m$. The problem can be reduced to some other celestial models proposed in the past like Copenhagen case (ν=2, β=0), Marañhao's four-body problem [27] (Figure 2a) and Ollöngren's restricted five- body problem [28] (Figure 2b), by simply adjusting the parameters.

2.1. Equations of motion

The motion of the particle is described in a synodic coordinate system by the following set of second order differential equations where all the quantities are dimensionless,

$$\begin{cases} \ddot{x} - 2\dot{y} = \dfrac{\partial U}{\partial x} = U_x, \\ \ddot{y} + 2\dot{x} = \dfrac{\partial U}{\partial y} = U_y, \\ \ddot{z} = \dfrac{\partial U}{\partial z} = U_z. \end{cases} \tag{1}$$

Where,

$$U = \frac{1}{2}\left(x^2 + y^2\right) + \frac{1}{\Delta}\left[\frac{\beta}{r_0} + \sum_{i=1}^{\nu} \frac{1}{r_i}\right], \tag{2}$$

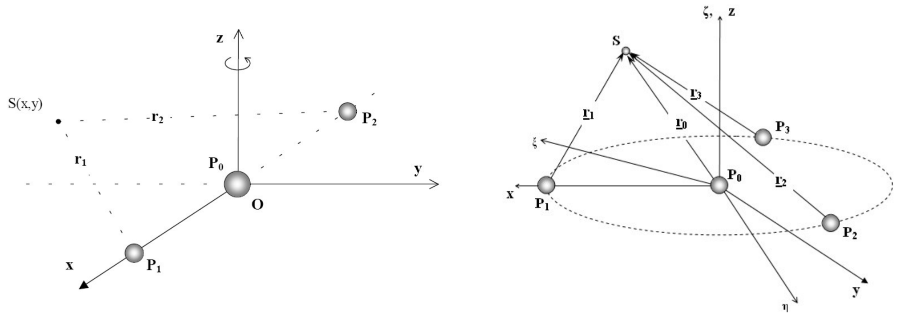

(a) (b)

Figure 2: (a) Marañhao's model ($\nu = 2, \beta \neq 0$), (b) Ollöngren's configuration ($\nu = 3, \beta \neq 0$).

is the effective potential and

$$r_0 = \left(x^2 + y^2 + z^2\right)^{1/2} \; r_i = \left[(x_i - x)^2 + (y_i - y)^2 + z^2\right]^{1/2},$$

are the distances of the particle from the primaries. We also have,

$$\Delta = M\left(\Lambda + \beta M^2\right) \quad \Lambda = \sum_{i=2}^{\nu} \frac{\sin^2(\pi/\nu)}{\sin[(i-1)(\pi/\nu)]} \quad M = 2\sin(\pi/\nu). \tag{3}$$

There is a Jacobian-type integral of motion where C is a constant.

$$C = 2U(x, y, z) - \left(\dot{x}^2 + \dot{y}^2 + \dot{z}^2\right). \tag{4}$$

2.2. Regions of allowed particle planar motions- Zero-velocity curves and $C = C(x, y)$ surfaces

In the planar motion these regions are limited by the zero-velocity curves (*zvc*) which are drawn by means of (3) and separate, for each value of C, the xy-plane in domains where motion is permitted from those where motion does not exist (Figure 3a). In the white almost circular areas which encircle the primaries, the motion of the particle is trapped. By considering a third axis which counts the values of the Jacobian constant C, we obtain, for each zero-velocity diagram, a corresponding three-dimensional plot and $C = C(x, y)$ called zero-velocity surface of particle's planar motion (Figure 3b). Motion is permitted inside the funnels and under the surface. Regarding the three-dimensional motion the zero-velocity surfaces (*zvs*) limit the domains of xyz-space in which motion is permitted from those where motion is not allowed. For example, in Figure 3c, motion is allowed and trapped inside the small almost spherical surfaces and is free outside the hyperboloid surface which encloses them. In Figure 3d the motion is trapped inside the central closed surface and inside the toroidal closed surface which surrounds all peripheral primaries, while it is free outside the hyperboloid envelop.

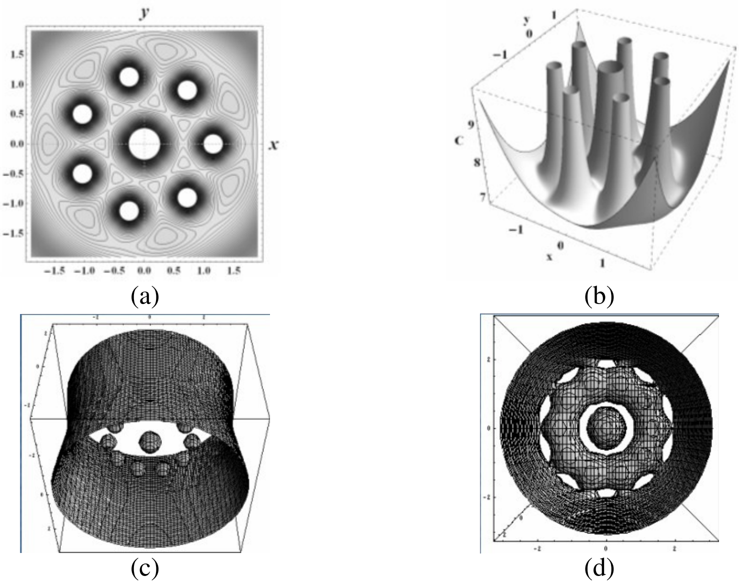

Figure 3: (a)-(b) Planar motion, $\nu = 7, \beta = 2$. Network of zero-velocity contours and zero-velocity surface $C = C(x, y)$. (c)-(d) $3D$ motion, $\nu = 10, \beta = 2$. Two “snapshots” of the evolution of the zero-velocity surfaces.

2.3. Equilibrium positions and equilibrium zones. Stability

The equilibrium positions in the gravitational case are all located on the xy-plane and are arranged on imaginary circles concentric to the one of the peripheral primaries which we call equilibrium zones. Their distribution preserves the symmetry of the configuration which repeats itself through rotations about the z-axis with an angle $2\pi/\nu$. The equilibria are grouped on either five (C_{A1}, C_{A2}, C_B, C_{C2}, C_{C1}) or three (C_{A1}, C_{C2}, C_{C1}) equilibrium zones and the equilibria of each zone are dynamically equivalent. These points are also located on the lines which either: (a) connect the central primary to a peripheral one and are called collinear (like those of zones A_1 and C_1), or (b) bisect the angles formed by the central primary and two consecutive peripheral ones and are called triangular (like those of zones A_2, B, C_2). For each ν there is a unique marginal value of $\beta = l_\nu$ at which a transition (bifurcation) from five to three equilibrium zones occurs. This value increases as ν increases. As β increases, the existing equilibrium zones approach from both sides the imaginary circle of the primaries. The Jacobian constants C of the equilibria play an important role since they determine the way that zero-velocity curves and surfaces evolve. Bifurcations in the topology of the *zvc* and *zvs* occur at values $C = C_W$, where $C_W = C_{A1}, C_{A2}, C_B, C_{C2}, C_{C1}$. Therefore, if $\beta < l_\nu$ five bifurcations occur, while if $\beta > l_\nu$ three bifurcations take place. All the equilibria for any combination of the two parameters ν and β are unstable.

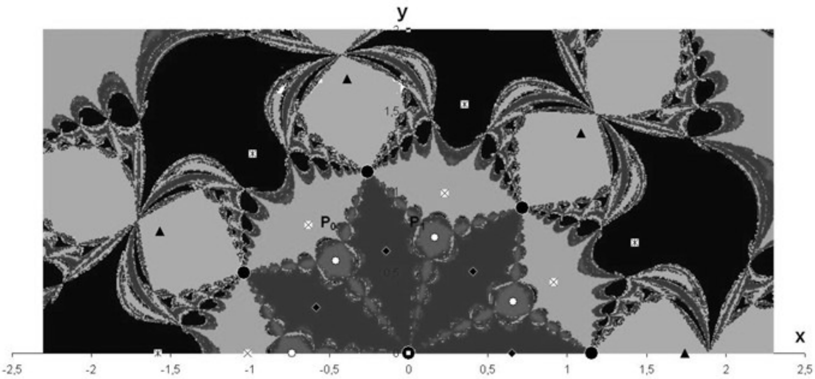

Figure 4: Attracting domains in the Newtonian case ($\nu = 7, \beta = 2$): A_1 (very dark grey), A_2 (dark grey), B (light grey), C_2 (black), C_1 (very light grey).

2.4. Attracting domains of the equilibria

An attracting domain is a set consisting of the initial points for which the application of an iterative process (in this case the Newton-Raphson algorithm) leads to the equilibrium positions of an equilibrium zone [7]. The domain of each zone presents all the symmetry elements of the primaries' arrangement. It generally consists of some "compact" parts, all the points of which lead to the equilibrium positions of this particular zone (Figure 4). Furthermore, we have found dispersed points that lie on the boundaries of the "compact" regions of this or other zones. These boundaries are not clearly defined and their distribution is rather chaotic. As regards the "speed" of convergence, we must note that the areas corresponding to fast convergence (within 1-5 steps) consist of the central "compact" parts of the attracting domains of the specific zone that surround the equilibrium positions of this zone and few dispersed points that frame these areas, but also appear near other equilibrium zones. As parameter β increases, the "compact" areas in general shrink and the number of the dispersed points of this class considerably decreases.

2.5. Planar and 3D periodic orbits and families. Stability

Periodic orbits are either simple or multiple and simple or multiple symmetric with respect to a coordinate axis. They are also characterized as direct or retrograde if they are described in the same or opposite sense to the rotation of the synodic coordinate system respectively. The orbits are grouped in families and those which are symmetric with respect to the x-axis are represented as single curves in a two-dimensional diagram (x_0, C) and are called characteristic curves [21, 8]. Some families evolve inside the funnels formed by the zero-velocity boundaries which surround the primaries (Figure 5a). They consist of planetary or satellite-type type orbits. Their characteristic curves have regions of stability (horizontal) and instability. Some other families emanate from the equilibrium points or bifurcate from families of the same multiplicity. As β increases, the characteristic curves shift towards the peripheral primaries and accumulate near their imaginary circle.

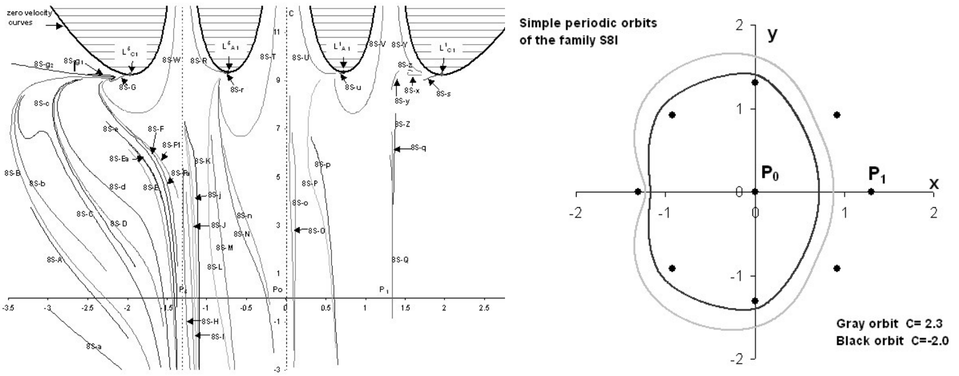

(a) (b)

Figure 5: (a) Families of s.p.orbits for $\nu = 8, \beta = 2$, (b) two interplanetary s.p.orbits.

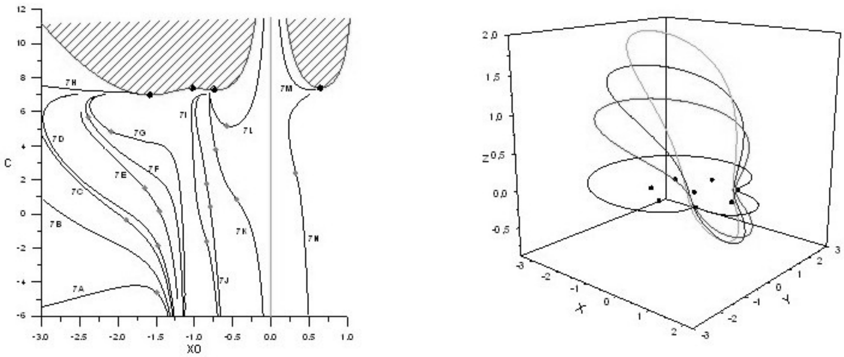

(a) (b)

Figure 6: $\nu = 7, \beta = 2$. (a) Vertical critical points from planar to $3D$ orbits, (b) a family of $3D$ periodic orbits.

Regarding the three dimensional motions we have found that only orbits symmetric with respect to the xz-plane may exist [15]. Figure 6a shows how the families of planar periodic orbits emanate from the fixed points (black circles) in the case where $\nu = 7$ and $\beta = 2$. The shaded regions are forbidden areas for particle's motion. The bifurcation points from the planar to the three-dimensional families of periodic orbits are shown with small grey triangles (vertical critical points) and they are located in the stability regions of the characteristic curves. The parametric research shows that the dynamics of the three-dimensional ring problem remains qualitatively the same, regardless how massive is the central primary with respect to the other primaries.

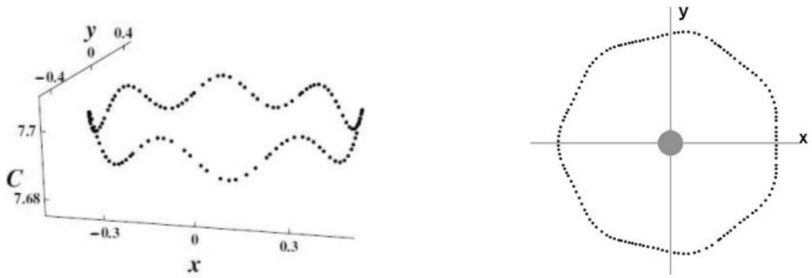

(a) (b)

Figure 7: $\nu = 7, \beta = 2$. (a) Focal curve in xyC space, (b) projection of this curve on xy-plane.

2.6. Focal points and focal curves, a new property

In addition to the known general properties of the zero-velocity curves and surfaces a new property has been proved in the particular ring problem [19]. In simple words, the $C = C(x, y)$ surfaces drawn for a particular ν and various values of β intersect along a unique wavy curve,

$$\sum_{i=1}^{\nu} \frac{r_0}{r_i} = \frac{1}{4} \sum_{i=2}^{\nu} \frac{1}{\sin(i - \pi/\nu)}, \tag{5}$$

whatever is the value of the mass parameter β. This curve surrounds the central primary (Figure 7) and as a consequence of this, the zero-velocity curves of the diagrams, that are drawn for $y = 0$, for a particular ν and for various values of β, have two common points, which are symmetric with respect to the C axis when ν is even, and non-symmetric when ν is odd.

§3. Various versions of the original problem

3.1. The photo-gravitational regular polygon problem of (N+1) bodies

We use the basic principles of Radzievskii's theory. Briefly speaking, we assume that radiation influences the motion of the small body but does not affect the motion of the other primaries and that this force is expressed by a reduction factor $q = 1 - b$, where b is the radiation coefficient and is the ratio of force F_r caused by radiation to force F_g that results from gravitation. For an illuminating body with a given luminosity and mass this coefficient depends on the physical and geometrical characteristics of the illuminated particle. We also assume that the particle is very small and moves with velocities much smaller than the speed of light. Under these circumstances the effective potential has the general form,

$$U = \frac{1}{2}\left(x^2 + y^2\right) + \frac{1}{\Delta}\left[\frac{\beta q_0}{r_0} + \sum_{i=1}^{\nu} \frac{q_i}{r_i}\right], \tag{6}$$

[17, 22, 24, 1]. If $q = 0$, the radiation force balances the gravitational one, if $q < 0$, radiation surpasses gravity and if $q > 0$, the gravitational force exceeds radiation. In Figure 8 we depict the parametric distribution of the equilibrium points in two configurations.

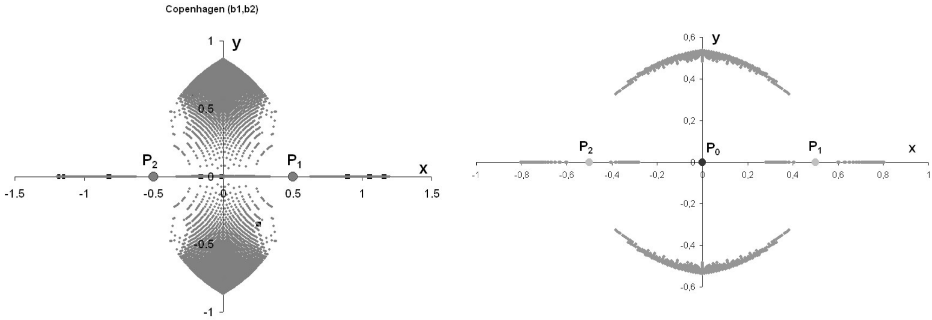

(a) (b)

Figure 8: (a) Copenhagen case where both primaries P_1 and P_2 radiate, (b) Marañhao's problem where the two peripheral primaries P_1 and P_2 radiate.

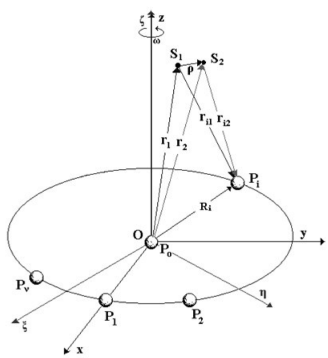

Figure 9: The regular polygon problem of $(N + 2)$ bodies.

3.2. The regular polygon problem of (N+2) bodies

In this version we consider two small interacting bodies instead of one (Figure 9). Then, in excess to the two parameters of the original gravitational case there are two parameters which are the reduced masses of the minor bodies S_1, S_2, $\mu_\alpha = m_\alpha/m$, $\alpha = 1, 2$. The model could simulate either dual satellite missions or two satellites in flying formation. The version is based on a combination of the 2 + 2 body problem [34] and the regular polygon problem of $(N + 1)$ bodies. We have studied the equilibrium points and their parametric variation [10] and we have found among other characteristics that each equilibrium point of the gravitational version belonging to zones A_1 and C_1 splits into two pairs of equilibria of S_1, S_2 on the same direction with these points, each equilibrium of zones A_2 and C_2 splits into four pairs which are located on the same direction and on a vertical direction and finally each equilibrium of zone B splits into two pairs located on a direction which is perpendicular to the direction of the initial points (Figure 10).

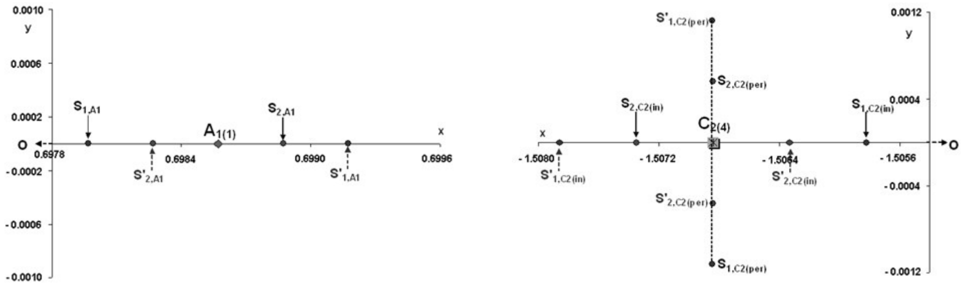

(a) (b)

Figure 10: (a) Two collinear pairs evolve around an equilibrium position of A_1 (or C_1), (b) four pairs (two collinear and two perpendicular) evolve around an equilibrium position of C_2 (or A_2).

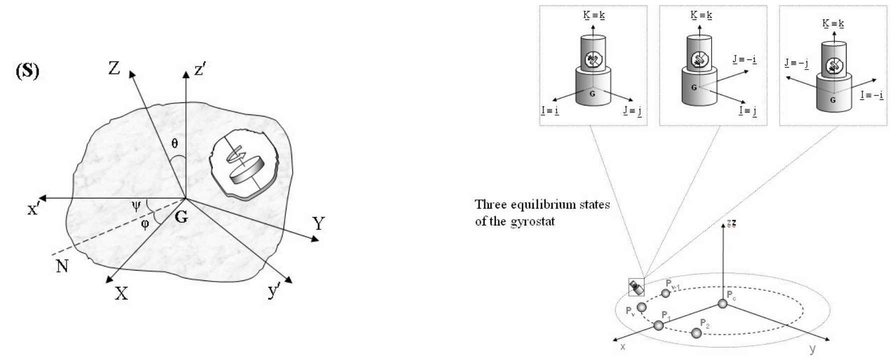

(a) (b)

Figure 11: (a) The structure of a one-rotor gyrostat, (b) three equilibrium states of the small gyrostat S in a regular polygon configuration.

3.3. The regular polygon problem of $(N+1)$ bodies where the small body is a gyrostat or a rigid body

A gyrostat consists of a platform or carrier and a number of rotors that are rigidly attached to it. Each rotor is spinning independently about an axis fixed on the platform and its motion does not modify the mass distribution of the gyrostat. A gyrostat is generally characterized by $(n+1)$ angular velocities, the n of which are the angular velocities of the spinning rotors relative to the platform. There are many fields of applications, e.g. artificial satellites, space-based telescopes and stations, etc. In this case we have investigated the existing equilibrium states of a one rotor-gyrostat [32] and of a tri-axial rigid body. The potential and the kinetic energy are expressed by means of the six independent variables x, y, z, ψ (angle of precession), θ (angle of nutation) and ϕ (angle of spin) (Figure 11a) and the small body's motion is described by a set of six second order differential equations describing the rotational and the translational component of motion. An equilibrium state is stable if both the translational and the rotational conditions ensure its stability (Figure 11b). A similar study was done in the case where the small body is a tri-axial rigid one [25].

3.4. The regular polygon problem of $(N + 1)$ bodies with Manev-like post-Newtonian potentials

Here we use a corrective term of the form B/r^3 in Newton's inverse square law of gravitation [26] which is related with the force field of the central primary. We try in this way to approximate either its non-sphericity (oblate or prolate body) or an existing radiation emission [2, 4, 11, 12, 13]. In this case a new parameter e is added to the two ones which appear in the conventional gravitational case. Although there are no significant qualitative changes if $e > 0$ (oblate body), however, important changes occur when this parameter is negative (prolate body). Figure 12a shows the zero-velocity surface for $\nu = 7, \beta = 2, e = -0.1$ and in Figure 12b the detail of the inversed central "chimney". In Figures 12c and d we depict the bifurcation diagram of the planar equilibrium positions and the out-of-plane equilibria respectively when $e < 0$. The distribution of the families of simple and double periodic orbits for $\nu = 7, \beta = 5$ and $e < -0.1$ are shown respectively in Figures 12e, f.

§4. Recent work and works in progress

4.1. The Copenhagen problem with Manev-like post-Newtonian quasi-homogeneous potentials

The gravitational version of this problem was first studied by Strömgren and colleagues between 1913 and 1939. The scientific interest focused again on this problem after the discovery of a great number of exosolar systems. During the last decade we treated some versions of it by considering that the small body is a triaxial rigid body or a gyrostat, as well as by assuming that the two primaries are radiation sources or magnetic dipoles [20, 23, 14], etc. Here we consider that the two major bodies create post-Newtonian Manev-type potentials. We studied the equilibrium points and we have found that when $e > 0$ there are only the five equilibrium Lagrangian points of the gravitational case, while when $-0.5 < e < 0$, in excess of these, 20 different new unstable equilibrium points (Figure 13a) may appear. We also investigated the symmetric periodic orbits (simple or multiple) and the evolution of their families. Many families evolve in the permitted areas between the inversed parts of the "chimneys" and the external parts of them and consist of satellite-type simple periodic orbits which emanate from the equilibrium points L_{E1}, L_{E2}, L_{E3} and L_{E4} and bifurcate to families with the same or higher multiplicity (Figures 13b). Other families emanate from the collinear Lagrangian points L_1, L_2 and L_3. The motion of the particle may be trapped for certain values of the Jacobian constant C in some regions of the xy plane or move freely on the xy-plane for other values of this constant ($C < C_{L2}$).

4.2. Works in progress

Trying to improve or to extend the regular polygon model we are now investigating some new versions; (i) the regular polygon problem of $(N + 1)$ bodies with Schwarzschild-like

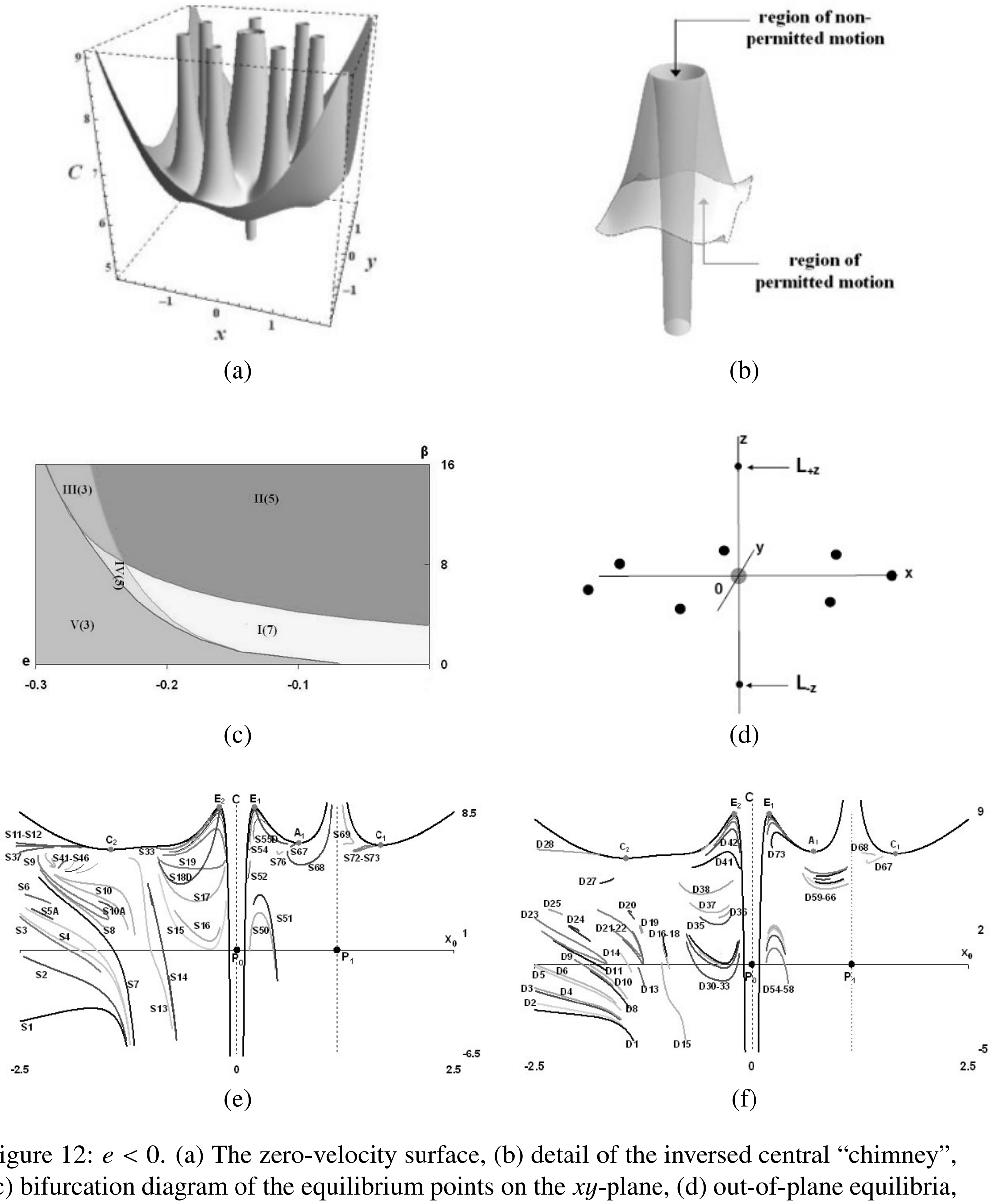

Figure 12: $e < 0$. (a) The zero-velocity surface, (b) detail of the inversed central "chimney", (c) bifurcation diagram of the equilibrium points on the xy-plane, (d) out-of-plane equilibria, (e)-(f) families of simple and double per.orbits for $\nu = 7, \beta = 5, e = -0.1$.

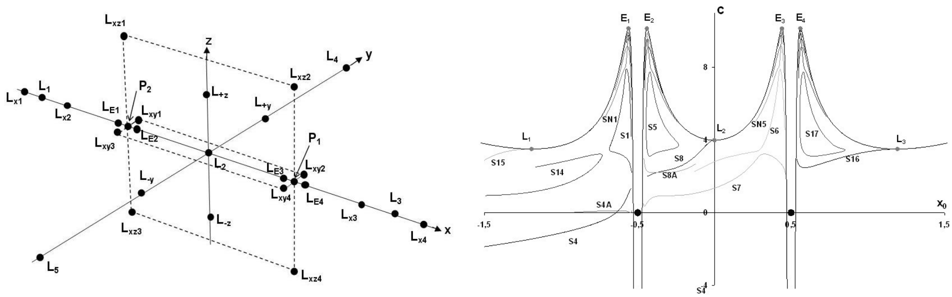

(a) (b)

Figure 13: (a) Distribution of the existing equilibria when $e < 0$, (b) families of simple periodic orbits for $e = -0.03$.

quasi-homogeneous potentials, (ii) the regular polygon problem of $(N + 2)$ bodies where all primaries are radiation sources or create post-Newtonian quasi-homogeneous potentials.

References

[1] Arribas, M., Abad, A., Elipe, A., and Palacios, M. Out-of-plane equilibria in the symmetric collinear four-body problem with radiations pressure. *Astrophys. Space Sci. 361* (2016), 270.

[2] Arribas, M., and Elipe, A. Bifurcations and equilibria in the extended N-body problem. *Mech. Res. Comm. 31* (2004), 1–8.

[3] Arribas, M., Elipe, A., Kalvouridis, T. J., and Palacios, M. Homographic solutions in the planar $(n+1)$ problem in a quasi- homogeneous potential. *Celest. Mech. Dyn.Astron. 99*, No1 (2007), 1–12.

[4] Arribas, M., Elipe, A., and Palacios, M. Linear stability of ring systems with generalized central forces. *Astron. Astrophys. 489* (2008), 819–824.

[5] Bang, D., and Elmabsout, B. Restricted $N + 1$-body problem: Existence and stability of relative equilibria. *Celest. Mech. Dyn. Astron. 89* (2004), 305–318.

[6] Barrio, R., Blesa, F., and Serrano, S. Qualitative analysis of the $(N + 1)$-body ring problem. *Chaos, Solitons and Fractals 36* (2008), 1067–1088.

[7] Croustalloudi, M. N., and Kalvouridis, T. J. Attracting domains in ring-type N-body formations. *Planetary and Space Sci. 55*, No 1-2 (2007), 53–69.

[8] Croustalloudi, M. N., and Kalvouridis, T. J. Periodic motions of a small body in the newtonian field of a regular polygonal configuration of $(\nu + 1)$ bodies. *Astrophys. Sp. Sci. 314* (2008), 7–18.

[9] Croustalloudi, M. N., and Kalvouridis, T. J. Regions of a satellite's motion in a Maxwell's ring system of N bodies. *Astrophys. Sp. Sci. 331* (2011), 497–510.

[10] Croustalloudi, M. N., and Kalvouridis, T. J. The regular polygon problem of $(N+2)$ bodies: a numerical investigation of the equilibrium states of the minor bodies. *Astrophys. Sp. Sci. 355*, No 1 (2015), 57–67.

[11] Elipe, A., Arribas, M., and Kalvouridis, T. J. Periodic solutions and their parametric evolution in the planar case of the $(n+1)$ ring problem with oblateness. *Journal of Guidance, Control and Dynamics 30*, No 6 (2007), 1640–1648.

[12] Fakis, D. G., and Kalvouridis, T. J. Dynamics of a small body in a maxwell ring-type N-body system with a spheroid central body. *Celest. Mech. Dyn. Astr. 116*, No 3 (2013), 229–240.

[13] Fakis, D. G., and Kalvouridis, T. J. On a property of the zero-velocity curves and surfaces in the regular polygon problem of $(N+1)$ bodies with a quasi-homogeneous potential. *Rom. Astr.J. 24*, No 1 (2014), 7–26.

[14] Fakis, D. G., and Kalvouridis, T. J. The Copenhagen problem with a quasi-homogeneous potential. (subm.).

[15] Hadjifotinou, K. G., and Kalvouridis, T. J. Numerical investigation of periodic motion in the three-dimensional ring problem of n bodies. *International Journal of Bifurcation and Chaos 15* (2005), 2681–2688.

[16] Kalvouridis, T. J. A planar case of the $(N+1)$ body problem: the 'ring' problem. *Astrophys. Sp. Sci. 260*, No 3 (1999), 309–325.

[17] Kalvouridis, T. J. The effect of radiation pressure on the particle dynamics in ring type N-body configurations. *Earth, Moon and Planets 87*, No 2 (2001), 87–102.

[18] Kalvouridis, T. J. Zero velocity surfaces in the three-dimensional ring problem of $N+1$ bodies. *Celest. Mech. Dyn. Astron. 80* (2001), 133–144.

[19] Kalvouridis, T. J. On a property of zero-velocity curves in N-body ring-type systems. *Planetary and Space Science 52* (2004), 909–914.

[20] Kalvouridis, T. J. On some new aspects of the photo-gravitational Copenhagen problem. *Astrophys. Sp. Sci. 317*, No 1-2 (2008), 107–117.

[21] Kalvouridis, T. J. Particle motions in Maxwell's ring dynamical systems. *Celest. Mech. Dyn. Astron. 102*, No 1-3 (2008), 191–206.

[22] Kalvouridis, T. J., Arribas, M., and Elipe, A. Dynamical properties of the resticted four-body problem with radiation pressure. *Mech. Res. Comm. 33*, No 6 (2006), 811–817.

[23] Kalvouridis, T. J., and Gousidou-Koutita, M. Basins of attraction in the Copenhagen problem where the primaries are magnetic dipoles. *Applied Mathematics 3*, No 6 (2012), 541–548.

[24] Kalvouridis, T. J., and Hadjifotinou, K. G. Bifurcations from planar to three-dimensional periodic orbits in the photo-gravitational restricted four-body problem. *Inter. J. of Bifurcation and Chaos 18*, No 2 (2008), 465–479.

[25] Kalvouridis, T. J., and Tsogas, V. Rigid body dynamics in the restricted ring problem of $(N+1)$ bodies. *Astrophys. Sp. Sci. 282*, No 4 (2002), 751–765.

[26] Maneff, G. La gravitation et le principe de l'action et de la reaction. *C. R. Acad. Sci. Paris 178* (1924), 2159–2161.

[27] Marañhao, D. L. *Estudi del flux d'un problema restringit de quatre cossos*. PhD thesis, Universitat Autonoma de Barcelona, 1995.

[28] Ollöngren, A. On a particular restricted five-body problem, an analysis with computer algebra. *J. Symbolic Comput. 6* (1988), 117–126.

[29] Papadakis, K. E. Asymptotic orbits in the $(N + 1)$-body ring problem. *Astrophys. Sp. Sci. 323* (2009), 261–272.

[30] Salo, H., and Yoder, C. F. The dynamics of co-orbital satellite systems. *Astron. Astrophys. 205* (1988), 309–327.

[31] Scheeres, D. *On symmetric central configurations with application to satellite motion about rings*. PhD thesis, The University of Michigan, USA, 1992.

[32] Tsogas, V., T.J.Kalvouridis, T. J., and Mavraganis, A. G. Equilibrium states of a gyrostat satellite moving in the gravitational field of an annular configuration of N big bodies. *Acta Mechanica 175*, No 1-4 (2005), 181–195.

[33] Vanderbei, R. J., and Kolemen, E. Linear stability of ring systems. *Astron. J. 133* (2007), 656–664.

[34] Whipple, A. Equilibrium solutions of the restricted problem of 2 + 2 bodies. *Celest. Mech. Dyn. Astr. 33* (1984), 271–294.

Tilemachos Kalvouridis
Dept. of Mechanics, National Technical University of Athens
5, Heroes of Politechnion Ave., 15773, Greece
tkalvouridis@gmail.com